



Missouri University of Science and Technology  
Scholars' Mine

---

International Conferences on Recent Advances in Geotechnical Earthquake Engineering and Soil Dynamics 1995 - Third International Conference on Recent Advances in Geotechnical Earthquake Engineering & Soil Dynamics

---

04 Apr 1995, 2:30 pm - 3:30 pm

## Seismic Response of 20-Valleys: Local Site Effects

K. E. Loukakis

*National Technical University, Athens, Greece*

J. Bielak

*Carnegie-Mellon University, Pittsburgh, Pennsylvania*

Follow this and additional works at: <https://scholarsmine.mst.edu/icrageesd>

 Part of the [Geotechnical Engineering Commons](#)

---

### Recommended Citation

Loukakis, K. E. and Bielak, J., "Seismic Response of 20-Valleys: Local Site Effects" (1995). *International Conferences on Recent Advances in Geotechnical Earthquake Engineering and Soil Dynamics*. 11. <https://scholarsmine.mst.edu/icrageesd/03icrageesd/session07/11>

This Article - Conference proceedings is brought to you for free and open access by Scholars' Mine. It has been accepted for inclusion in International Conferences on Recent Advances in Geotechnical Earthquake Engineering and Soil Dynamics by an authorized administrator of Scholars' Mine. This work is protected by U. S. Copyright Law. Unauthorized use including reproduction for redistribution requires the permission of the copyright holder. For more information, please contact [scholarsmine@mst.edu](mailto:scholarsmine@mst.edu).

## Seismic Response of 2D-Valleys: Local Site Effects

Paper No. 7.21

**K.E. Loukakis**

Research Assistant, Civil Engineering Dept., National  
Technical University, Athens, Greece

**J. Bielak**

Professor, Civil Engineering Dept., Carnegie-Mellon  
University, Pittsburgh, Pennsylvania

**SYNOPSIS** Layering and geometry effects on ground response of two-dimensional sedimentary valleys under oblique seismic excitation are investigated. The seismic wave has the shape of a half cycle incoming pulse with SV-wave characteristics. Vertical and oblique incoming signals of varying duration are used. The analysis is performed using finite element techniques, an equivalent effective force method to prescribe the free field motion within the domain of computation, and an artificial boundary to absorb the scattered motion. Simple examples are presented confirming the validity of this methodology. It is shown that surface waves generated at the valley edges propagate through the basin producing an increased ground response. Horizontal and vertical displacements are affected significantly by valley geometry, particularly by the inclination of the valley sides. Layering and inclined waves contribute to producing amplification and very long duration of ground motion.

### INTRODUCTION

Soft surface layers laterally confined in the form of sediment-filled valleys or basins are oftentimes the cause of large amplifications and variations of seismically induced ground motion. Two- or three-dimensional models are frequently required to apprehend the effects of geometric and material irregularities on ground response and to effectively predict the observed motion.

The authors have previously presented results of two-dimensional analysis of homogeneous and layered valleys subjected to SV-waves (1994a, and 1994b). These studies focused on the effects of layering and material damping on ground response. It was shown that the edge of the valley generates surface (Rayleigh) waves which are trapped between the two edges and increase the amplitude of the motion as well as its duration. These effects are more pronounced for layered valleys. Damping has the effect of reducing surface wave effects in homogeneous valleys. However, damped response of layered valleys is still characterized by increased ground response, especially if the angle of incidence is nearly critical. At this angle, the horizontal component of slowness of S-waves matches the P-wave slowness, and a strong coupling occurs, including the generation of surface waves and large amplitudes of the ground surface.

Several methods have been used for analyzing the seismic response of sedimentary valleys. These include finite differences, finite elements, ray techniques, Aki-Larner, discrete wavenumber, and boundary integral methods as summarized by Aki (1988). In this work we make use of the finite element method, which has the important feature of enabling one to model valleys of arbitrary shape with regular or irregular layers and arbitrary inclusions. The material can be heterogeneous, and even nonlinear (elastic or inelastic). An absorbing boundary is used to render finite the domain of computation, and an effective force method to prescribe the free field motion within the finite element mesh.

Our methodology is first illustrated with two

examples. The first one portrays SV-wave propagation through homogeneous halfspace, whereas the second one validates the performance of the absorbing boundary. The role that geometry and layering within a valley play on surface ground motion under oblique SV-wave excitation is explored subsequently.

### FINITE ELEMENT MODELLING

Two important issues must be addressed if one is to use finite elements for modeling seismic motion in unbounded domains. One concerns the need to limit the domain of computation. A great deal of attention has been given in recent years to developing efficient artificial boundaries. In this work we shall use, for convenience, the simple dashpots proposed by Lysmer and Kuhlemeyer (1969). As will be seen, these dashpots give satisfactory results for the cases considered here.

The second point that requires attention is how to incorporate the excitation into the model if the earthquake source is located outside the domain of computation. To solve this problem by the finite element method we introduced a modified version of a procedure developed for treating soil-structure interaction systems subjected to arbitrary excitation. The problem was formulated by Bielak and Christiano (1984) and implemented by Cremonini et al (1988) using a domain decomposition technique in which the interior and exterior regions were considered separately. The interior is allowed to behave nonlinearly and represents the valley which may be layered and contain irregularities. The exterior representing the halfspace is constrained to be elastic or viscoelastic. In this application we consider only the linear case. The problem is to determine the total (plane) displacement field due to the incident wave, both inside the valley and on a small portion of the exterior region in the immediate vicinity of the valley.

In order to introduce the free-field excitation into the formulation, the problem is treated as one of diffraction in which the total displacements are

regarded as the unknowns within the valley, while only relative displacements, measured with respect to the free-field displacements, are the unknowns in the truncated halfspace. The model has been rendered finite by the introduction of an absorbing boundary characterized by appropriate viscous damping matrices. It is important to emphasize that the artificial boundary is only needed to absorb the scattered waves. Viscous damping may also be assigned to simulate material damping in the valley and the halfspace.

Our procedure consists in first writing the discretized equations of motion for the valley and the surrounding medium separately; one then uses the conditions of continuity of displacements and tractions across the halfspace-valley interface, together with the equations of motion for the nodal free-field displacements within the original halfspace to arrive at the final governing equations for the complete system. Details of the derivation are given in Loukakis (1988) and summarized in Loukakis and Bielak (1994a, and 1994b). Our methodology, can be applied equally well if the interior region is nonlinear since only the exterior is required to remain linear, and the effective seismic forces are applied only on the valley-halfspace interface and on exterior nodes immediately adjacent to this interface.

#### NUMERICAL EXAMPLES

Five models are selected to illustrate the effects of valley geometry and layering on the seismic response of shallow valleys due to transient oblique incident SV-waves. The valley models are shown in Figure 1. In Cases 1, 3, and 5 the valleys are filled with homogeneous material. In Cases 2 and 4 the model is subdivided into four homogeneous layers of equal thickness, and the shear wave velocity of each layer is such that the average shear wave velocity across the midsection is the same as the shear wave velocity of the homogeneous valley. Valleys of Cases 1 and 2 have horizontal base and sides inclined at 16.7 degrees, whereas in Cases 3 and 4 the sides are vertical. Case 5 has base sloping at 1.7 degrees and sides inclined at 16.7 degrees. The material properties for all five cases are listed in Table 1. In this table,  $\rho$ ,  $\nu$ ,  $C_s$ , and  $H$ , represent respectively, the density, Poisson's ratio, shear wave velocity, and thickness of each layer. Radiation damping in the system is taken into consideration by means of the absorbing boundary. Effects of material damping are neglected in this study.

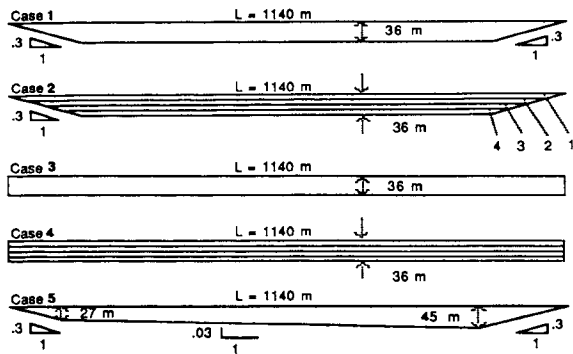


Figure 1. Valley Models

In all our examples the incident wave is defined by means of a single half cycle displacement pulse

with duration  $T$ , unit amplitude, and shape defined by Equation 1, which is transmitted as an oblique incident plane SV-wave, at an angle  $\theta_0$  with respect to the vertical.

Table 1. Material Properties

Units:  $\rho$  in  $\text{Kns}^2/\text{m}^4$ ;  $C_s$  in  $\text{m/s}$ ; and  $H$  in  $\text{m}$

Case	Layer 1				Layer 2				Layer 3				Layer 4				Halfspace					
	$\rho$	$\nu$	$C_s$	$H$	$\rho$	$\nu$	$C_s$	$H$	$\rho$	$\nu$	$C_s$	$H$	$\rho$	$\nu$	$C_s$	$H$	$\rho$	$\nu$	$C_s$			
1,3,5	2.5	0.4	70	36	-	-	-	-	-	-	-	-	-	-	-	-	-	-	2.8	0.3	400	
2,4	2.2	0.4	30	9	2.4	0.4	56.7	9	2.6	0.4	83.3	9	2.7	0.4	110	9	2.8	0.3	400			

$$\Phi(t) = 1 - 3\tau^2 + 3\tau^4 - \tau^6, \quad \tau = (2t - T)/T, \quad 0 \leq t \leq T \quad (1)$$

The total free field motion consists of the incident wave plus the reflected wave. Detailed expressions, are given in Loukakis (1988), for angles of incidence  $\theta_0$ , less than the critical value  $\theta_{cr}$ , for which there is total conversion of the incident SV-wave into a P reflected wave.  $\theta_{cr}$  depends exclusively on  $\nu$ , and for the value considered here ( $\nu=0.3$ ),  $\theta_{cr}=32.3^\circ$ . For angles greater than  $\theta_{cr}$  a dispersive surface wave is generated in the halfspace, except for  $\theta_0=45^\circ$ , in which case the incident wave is reflected as a pure SV wave.

The finite element mesh used to solve the wave propagation problem within the valley and a finite portion of the surrounding halfspace, together with the standard lumped viscous dampers used as an absorbing boundary, are shown on Figure 2.

For clarity, different scales have been used for the horizontal and vertical directions. The mesh consists of quadratic isoparametric 8-node rectangular and 6-node triangular elements. The excitation is applied at the nodes of the interface strip of triangular elements, as explained in the previous section. Calculations are extended over an interval of 20s or 30s, depending on the response of the valleys, with a time step of 0.025s for a pulse duration of 0.5s, and of 0.05s for longer pulses. The particular values of  $T$  considered herein were chosen so that the duration  $2T$  corresponding to a full cycle pulse would be near one of the lower resonant periods of the one-dimensional flat model corresponding to the middle part of the valley.

Before discussing the response of the different valleys, we verify the validity of our methodology. We consider first the wave propagation of an inclined SV-wave through a homogeneous halfspace for the pulse defined by Equation 1, for different durations ( $T=0.5, 1, 2.5\text{s}$ ) and angles of incidence ( $\theta_0=0^\circ, 15^\circ, 32.3^\circ, \text{ and } 45^\circ$ ). The halfspace is modelled by the finite element mesh shown in Figure 2, in which all the elements are assigned the values of the mass density, shear wave velocity, and Poisson's ratio corresponding to the halfspace of Table 1. The resulting displacement histories at selected surface nodal points corresponding to an incident pulse of 1s duration are shown on Figure 3 for two different angles of incidence.

Throughout this paper, solid lines denote horizontal displacements while vertical displacements are presented by dotted lines. The nodes are numbered consecutively from west to east as shown on Figure 2. It can be verified that the wave travels along the surface with an apparent velocity  $C_{sp} = C_s / \sin \theta_0$ , as expected, i.e., 1545 m/s and 800 m/s for  $\theta_0=15^\circ$  and  $30^\circ$ , respectively. The

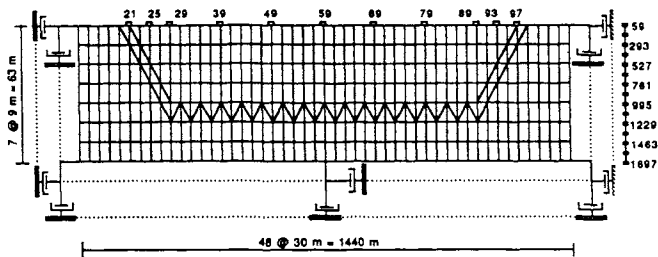
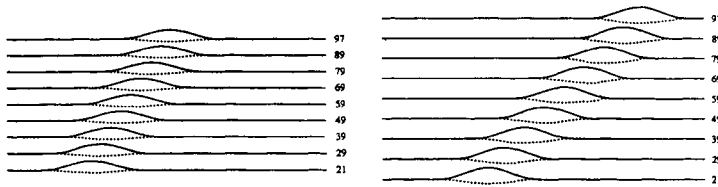


Figure 2. Finite Element Model



(a)  $\theta_0=15^\circ$

(b)  $\theta_0=30^\circ$

Figure 3. Nodal Displacement on Halfspace Surface

amplitude of the exact horizontal and vertical surface displacements are listed in Table 2, for several angles of incidence. For a halfspace, these displacements are independent of the duration of the pulse and of the shear wave velocity of the material. Values obtained from the finite element simulations for the various combinations of  $\theta_0$  and pulse duration of  $T=1s$  differed by less than 1 percent from the exact solutions, with the largest errors corresponding to the shortest pulses, as expected. Notice, that the amplitude of the displacement varies significantly with the angle of incidence  $\theta_0$ . The horizontal component reaches a maximum amplification of 4.35 at the free surface with respect to the amplitude of the incoming wave, for the critical angle, as opposed to a value of 2 for vertical incidence, while the vertical component vanishes for vertical incidence and increases at first with  $\theta_0$ ; the largest value occurs for  $\theta_0=30^\circ$ , it is small at critical incidence, and vanishes for  $45^\circ$  incidence.

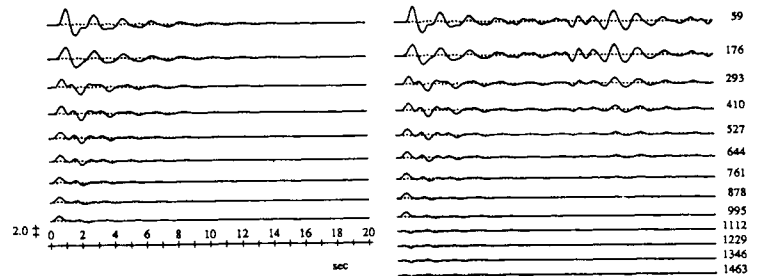
Table 2. Peak Nodal Displacements Halfspace Surface

	Angle of Incidence				
	$0^\circ$	$15^\circ$	$30^\circ$	$32.3^\circ$	$45^\circ$
Horizontal	2	1.99	2.41	4.35	1.41
Vertical	0	-0.56	-0.91	-0.15	0

It should be noted that in these examples the absorbing boundaries remain inactive since there is no scattered motion.

To illustrate the performance of the absorbing boundaries we consider next the response of the layered valley with stepped shear wave velocity (Case 2) depicted in Figure 1. Figure 4b shows the displacement history due to a vertically incident pulse of 1s duration. Figure 4a shows the corresponding records obtained by ignoring the effects of the lateral edges, that is for the corresponding one-dimensional system consisting of flat layers. Displacements at nodes below the valley bottom are not shown in this case. Notice that due to symmetry, motion occurs only in the horizontal direction, and that the difference between the two sets of records is due exclusively to the surface wave generated by the lateral edges. Surface wave effects will be discussed further separately. Now we concentrate on the response at the bottom of the valley and points below. Recall

that within the exterior region the displacements represent only the relative (scattered) motion with respect to the free-field displacement. Figure 4b shows that these relative displacements are small, indicating that the valley has only a small effect on the halfspace motion (e.g., Nodes 1112, 1229, 1346, 1463). The absence of noise in these records clearly indicates that the absorbing boundary is effective in transmitting this outgoing motion without generating spurious reflections.



(a) 1D-response

(b) 2D-response

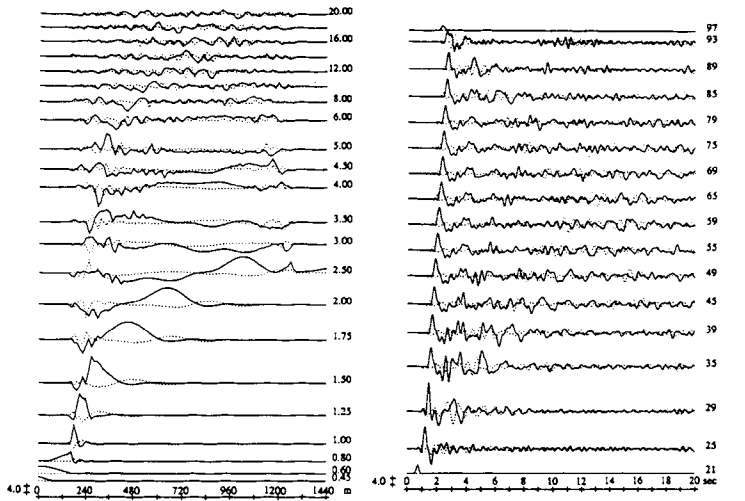
Figure 4. Nodal Displacements, Case 2,  $T=1s$ ,  $\theta_0=0^\circ$

We now turn to the free-surface response of the sedimentary valleys under study for various angles of incidence and durations of the incoming pulse.

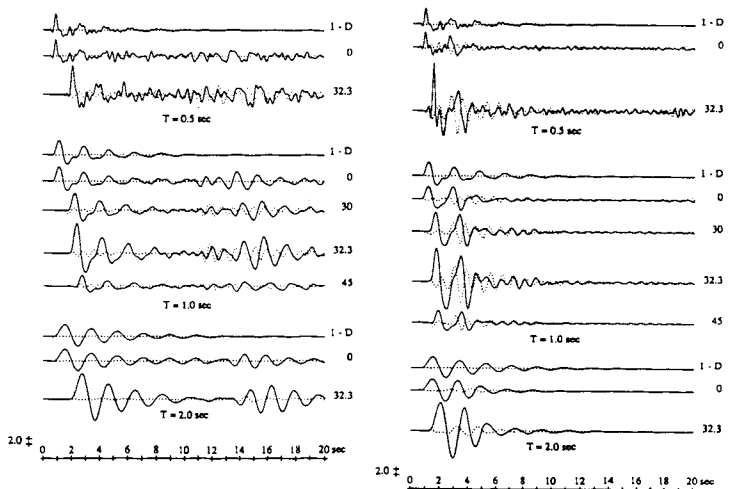
Figure 5 shows the response of Case 2 valley (shear wave velocity increasing stepwise with depth) to a 0.5s pulse at critical incidence. Figure 5a depicts the free surface profile at various times while the displacement traces at selected nodal points appear on Figure 5b. The profile includes the total valley free-surface as well as the part of the halfspace included within the domain of computation, for a total of 1140 m. Surface waves are generated at the valley western confluence as soon as the incident wave travelling through the halfspace reaches the free surface. The total response at points near the confluence (e.g., nodes 35, and 89) has a peak horizontal displacement that is of the same size or greater than the initial peak displacement due to the direct refracted waves even after 6s of motion. Near the center of the valley significant horizontal displacements are observed even after 16s of motion. The response on the left side of the valley is much greater than on the opposite side. This is an example of how seismic excitation moving in the direction of increasing layer thickness can lead to constructive interference, while the opposite is true if the seismic propagation is in the direction of decreasing layer thickness. The extremely large peak value of the horizontal displacement at node 29 for the case of critical incidence represents the most dramatic feature of the response. This peak horizontal displacement of 18.0 is 65 percent greater than the corresponding value at mid-valley (or flat-layered valley), which in turn is 2.5 times greater than the 4.35 amplitude in the free-field. Vertical displacements near the left confluence are particularly prominent. The spatial variation of the response near the valley confluences is especially pronounced; this variation can make long structures resting on multiple supports, such as bridges and pipelines, highly susceptible to damage during strong earthquakes.

The response of Case 2 valley to pulses of different duration and angles of incidence at two nodes, one in the middle of the valley (node 59) and the other near an edge (node 29) is shown on Figure 6. The free-surface displacement of the

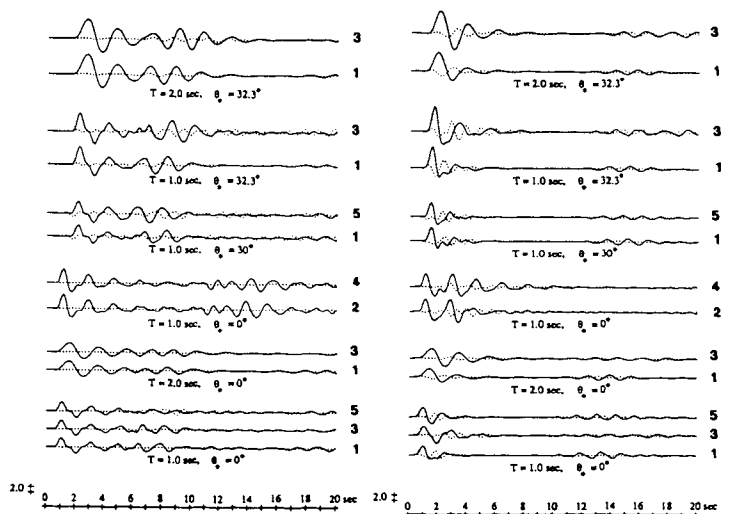
corresponding flat layered system due to a vertically incident pulse is also shown on Figure 6.



(a) Surface Profile(sec) (b) Nodal Displacements  
Figure 5. Case 2 Valley,  $T=0.5s$ ,  $\theta_{cr}=32.3^\circ$



(a) Middle Node (59) (b) Western Confluence (29)  
Figure 6. Case 2 Valley, different T and  $\theta$ .



(a) Middle Node (59) (b) Western Confluence (29)  
Figure 7. Geometry Effects, different T and  $\theta$ .

Increased duration and amplitude of response are the two most obvious effects due to lateral confinement. While surface wave effects are apparent at all angles of incidence, these are stronger for the critical angle.

Geometric effects on seismic response of two-dimensional valleys are illustrated on Figure 7. Ground motion at nodes 29 and 59 is presented for different pulse durations, and angles of incidence. A number (1 through 5) is assigned to each displacement history referring to the corresponding valley case of Figure 1. The horizontal component of the ground response of both homogeneous and layered valleys generally increases with increasing inclination of valley sides. Sloping valley base produces an increase in vertical ground response. The response of the valley with vertical sides at critical incidence is characterized by more pronounced surface wave effects. Near the confluence the valley response includes secondary horizontal and vertical peaks of the same amplitude.

#### CONCLUDING REMARKS

Finite element method provides an efficient tool for the analysis of the earthquake response of shallow sediment filled valleys. Effects of layering and geometry on seismic response of valleys to a single half cycle SV pulse are investigated using an effective seismic excitation. Horizontal and vertical displacements are affected significantly by valley geometry. Valley edges give rise to surface waves that propagate into the basin, generally producing an increase in response. In addition inclined waves and layering contribute to produce significant and sometimes dramatic, amplification and very long duration of the resulting surface motion. Near the confluence, the amplitude of the horizontal displacement can be four times as large as that of the corresponding flat system. Very large vertical displacements are also observed. Such effects are smaller, though still noticeable further from the confluences.

#### REFERENCES

Aki, K. (1988) "Local Site Effects on Strong Ground Motion", Earthq. Engr. and Struct. Dyn. 5:103-155.  
 Bielak, J., and P. Christiano (1984) "On the Effective Seismic Input for Non-Linear Soil-Structure Interaction Systems", Earthquake Engr. and Struct. Dynamics 12: 107-119.  
 Cremonini, M.G., P. Christiano and J. Bielak (1985) "Implementation of Effective Seismic Input for Soil Structure Interaction Systems", Earthquake Engr. and Struct. Dynamics 16: 615-625.  
 Loukakis, K. (1988) "Transient Response of Shallow Layered Valleys for Inclined Incident SV Waves Calculated by the Finite Element Method", M.S. Carnegie-Mellon Univ. Pittsburgh.  
 Loukakis, K. and J. Bielak (1994a) "Layering and Damping Effects on Seismic Response of Sedimentary Valleys to Oblique Excitation", Proc. II: Earthquake Resistant Construction and Design, Berlin, 1:93-100.  
 Loukakis, K. and J. Bielak (1994b) "Seismic Response of Two-Dimensional Sediment-Filled Valleys to Oblique Incident SV-Waves Calculated by the Finite Element Method", Proc. V: National Conf. on Earthquake Engineering, Chicago, 3:25-34.  
 Lysmer, J. and R.L. Kuhlemeyer (1969) "Finite Dynamic Model for Infinite Media", Journal of the Engineering Mechanics Division 95: 859-877.